

Hadron Production at Forward Rapidity in Nuclear Collisions at RHIC

HONGYAN YANG FOR THE BRAHMS COLLABORATION

Department of Physics and Technology, University of Bergen, 5007 Bergen, Norway

Received Nov 30, 2005

The main experimental results obtained by the BRAHMS experiment at Relativistic Heavy Ion Collider (RHIC) for Au+Au collisions at $\sqrt{s_{NN}} = 62.4, 200 \text{ GeV}$ and d+Au collisions at $\sqrt{s_{NN}} = 200 \text{ GeV}$ are presented. The m_T spectra and the Gaussian-like rapidity densities of produced pions and kaons in Au+Au central collisions at $\sqrt{s_{NN}} = 200 \text{ GeV}$ are shown, and their rapidity densities are compared with results from models. The net-proton yield in the same system is compared with that from AGS and SPS energies to study the high energy collision scenario - transparency and stopping. The rapidity, energy and centrality dependence of the nuclear modification factors in both systems are compared with models to differentiate between the initial and final state effect.

PACS: 25.75.-q, 25.75.Nq, 25.40.-h, 13.75.Cs

Key words: relativistic heavy ion collisions, hadron production, net-proton, nuclear modification factor, Cronin effect, jet-quenching

1 Introduction

At RHIC energies, an extremely hot and dense matter is produced in ultra-relativistic heavy ion collisions, in which the so-called Quark Gluon Plasma (QGP) [1] might have been created. The hadrons produced in the relativistic heavy ion collisions provide a promising way to study the possible existence of that early color deconfined state of matter. In such collisions, the large number of the produced particles and their subsequent re-interactions, either at the partonic or hadronic level, motivates the application of concepts of fluid dynamics in their interpretation. Hydrodynamics properties of the expanding matter created in heavy ion collisions have been discussed by Landau [2] and Bjorken [3], which corresponds to the full stopping and transparency scenarios, in theoretical pictures using different initial conditions. The measurement on the net-proton production may give a test on both models at RHIC energies. In both scenarios, thermal equilibrium is quickly achieved and the subsequent isentropic expansion is governed by hydrodynamics. The yields and the kinematic properties of the produced hadrons provide an important tool to test whether equilibrium occurs in the collision.

On the other hand, the high p_T (above $2 \text{ GeV}/c$) hadrons are mainly produced in the initial hard scattering between the partons from colliding nuclei. When the hard scattered partons traverse through the medium, they will lose a large fraction of their energy by induced gluon radiation if the medium is QGP, which effectively leads to suppression of jet production, i. e. the so called jet-quenching [4]. Experimentally the depletion of the high p_T region in hadron spectra are expected if QGP is formed in the collision. The hadrons produced in d+Au collisions with high p_T

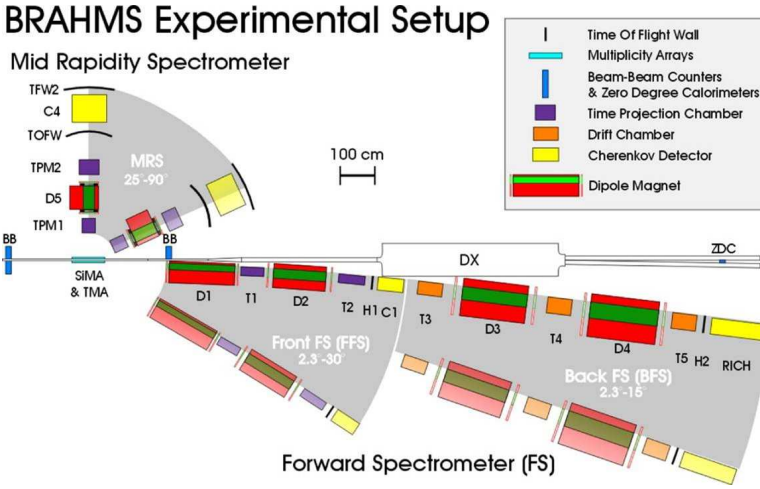


Fig. 1. Overview of the BRAHMS setup

will remain mostly unchanged before they are detected since the final state interactions are not expected to play a dominant role in such a small system [5]. The saturation of initial parton densities in relativistic heavy ion collisions, a manifestation of high-density QCD, is expected to significantly influence the pseudo-rapidity and centrality dependence of the emitted charged particle densities from these reactions. Therefore, the d+Au collisions provide us an ideal experimental method to disentangle initial and final state effects in heavy ion collisions.

2 Experimental setup and particle identification

BRAHMS, Broad RAnge Hadron Magnetic Spectrometers, one of the four detectors at RHIC, is located at the 2 o'clock experimental hall of the RHIC collider. It has two rotatable magnetic spectrometers with particle identification capabilities for hadrons, mid-rapidity spectrometer (MRS) and the forward spectrometer (FS), which gives the unique capability to study particle production in a broad range of both transverse momenta and rapidities. See the schematic layout of the experiment in Fig. 1.

The purpose of the mid-rapidity spectrometer (MRS) is to detect and identify the particles emitted at mid-rapidity. Particles at forward rapidities are detected by the Forward Spectrometer (FS). Both spectrometers have dipole magnets with tracking chambers located on each side of the magnet gaps. BRAHMS uses the Time-of-Flight (TOF) technique in both spectrometers, and a Ring Imaging Čerenkov (RICH) detector at the back of the FS for the identification of particles with high momentum. Fig. 2 shows the PID performance in Au+Au collisions by

the time-of-flight wall (TOFW) achieved in MRS (left panel) and RICH in FS (right panel). In MRS, pions and kaons can be separated up to $2.0 \text{ GeV}/c$ in momentum by the TOFW. The π - K separation by TOF in FS is up to $p = 4.5 \text{ GeV}/c$, and is further extended up to $20 \text{ GeV}/c$ by RICH. Details of the BRAHMS apparatus can be found in Ref. [6].

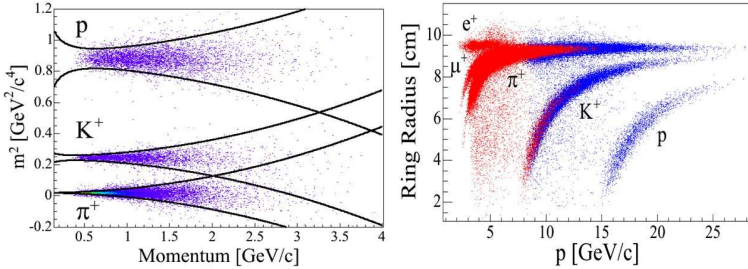


Fig. 2. Left: PID by TOFW in MRS, mass-squared as function of momentum. The curves indicate a $\pm 2\sigma$ cut around the pions, kaons and protons. Right: PID by RICH in FS, ring radius as function of momentum for two different magnet settings. The bands in the data correspond to electrons, muons, pions, kaons and protons.

The experimental method and the analysis techniques used to extract the spectra, which are used to construct the nuclear modification factors, are described in Ref. [7]. Each contribution was obtained from several magnetic field setting and corrected for the spectrometer acceptance, tracking efficiency and trigger efficiency.

3 Experimental results

3.1 Hadron production and stopping

Fig. 3 shows the transverse mass $m_T - m_0$ spectra ($m_T = \sqrt{p_T^2 + m^2}$) for π^- and K^- in 5% most central Au+Au collisions at $\sqrt{s_{NN}} = 200 \text{ GeV}$. Particle spectra were obtained by combining data from several spectrometer settings, each of which covers a small region of the phase-space ($y - p_T$). The data has been corrected for the limited acceptance of the spectrometers using a Monte Carlo calculation simulating the geometry and tracking of the BRAHMS detector system. Detector efficiency, multiple scattering and in-flight decay corrections have been estimated using the same technique. The data have not been corrected for feed-down from resonance and hyperon decays. Details can be found in Ref. [8] and references therein.

The pion spectra are well described at all rapidities by a power law in p_T , $A(1 + p_T/p_0)^{-n}$. For kaons, an exponential in $m_T - m_0$, $A \exp(m_T - m_0)/T$, has been used. The invariant yields dN/dy were calculated by integrating the fit functions over the full p_T or m_T range.

Fig. 4 shows the rapidity densities (panel (a)) and rapidity dependence of mean transverse momenta $\langle p_T \rangle$ (panel (b)), which are extracted from the fits of pions and

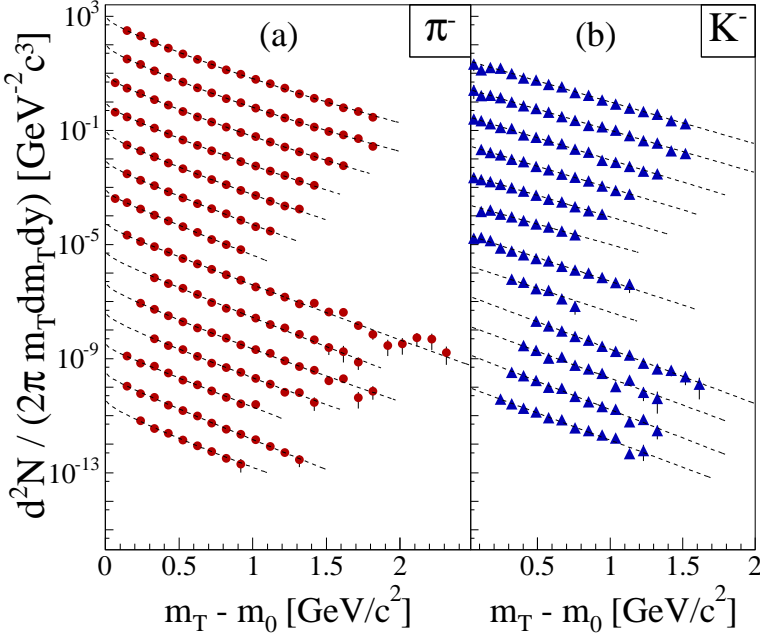


Fig. 3. Invariant transverse mass $m_T - m_0$ spectra for π^- (a) and K^- (b) from $y \sim 0$ (top) to $y \sim 3.5$ (bottom). Dashed lines are fits to the data. Errors are statistical only. Spectra have been rescaled by power of 10 for the successive rapidity bins.

kaons. The rapidity densities exhibit a nearly Gaussian shape. The widths of these Gaussians are found to be $\sigma_{\pi^+} = 2.27 \pm 0.02$ and $\sigma_{\pi^-} = 2.31 \pm 0.02$ rapidity units. In panel (b), no significant difference between positive and negative particles of a given mass is found, and a very slight change of $\langle p_T \rangle$ from mid-rapidity to forward rapidity is observed for both pions and kaons.

Similar overall features have already been observed in central Au+Au collisions at AGS [9] and Pb+Pb collisions at SPS [10]. This is reminiscent of the hydrodynamical expansion model proposed by Landau [2]. In initial state, colliding nuclei are highly Lorentz contracted along the beam direction. Under assumption of full stopping and isentropic expansion after the initial compression phase (where thermal equilibrium reached), the hydrodynamical equations, using the equation of state of a relativistic gas of massless particles lead to dN/dy distribution of Gaussian shape at freeze-out. In a simplified version of Landau model [11] developed for the description of particle production in p+p collisions, the width σ of the pion distribution is formulated as follows:

$$\sigma^2 = \ln \gamma_{beam} = \ln(\sqrt{s_{NN}}/2m_{proton}), \quad (1)$$

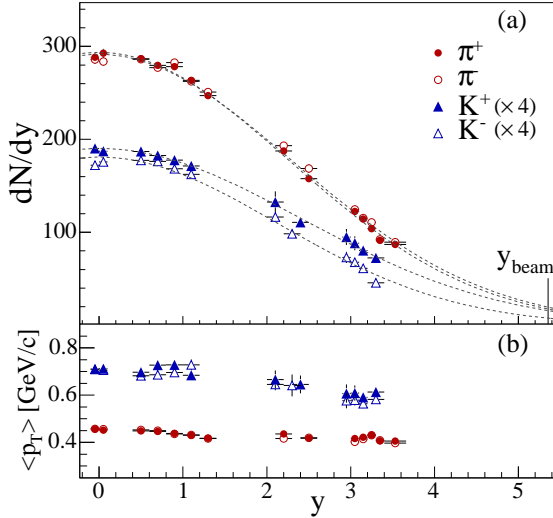


Fig. 4. Pion and kaon rapidity densities (a) and their mean transverse momentum $\langle p_T \rangle$ (b) as a function of rapidity. Errors are statistical. The dashed lines are the Gaussian fits to the dN/dy distributions.

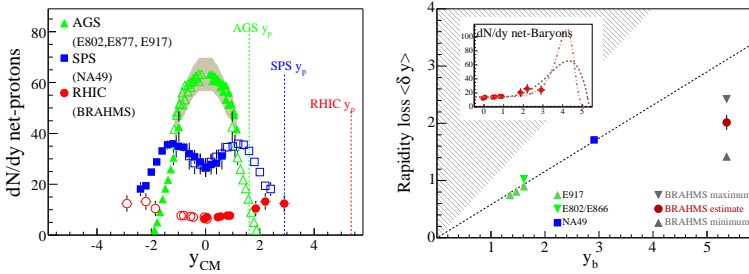


Fig. 5. Left: rapidity density of net protons measured at AGS, SPS and RHIC (BRAHMS) for central collisions. Right: The rapidity loss comparison at different energies. The inserted plot on the right panel is the estimation of possible net baryon distributions requiring baryon number conservation.

which gives $\sigma_{Landau} = 2.16$. Surprisingly, only a 5% discrepancy between the experimental width with the width estimated by the model is observed.

At RHIC energy, the net-proton density is much lower than that at AGS and SPS energies, see the left panel in Fig. 5. The rapidity loss, which is used to estimate the stopping power of a colliding system, which is defined by the difference between

the beam rapidity y_{beam} and its average rapidity after collision $\langle y \rangle$, namely $\delta y = y_{beam} - \langle y \rangle$, in which $\langle y \rangle$ is defined as

$$\langle y \rangle = \int_0^{y_{beam}} y \frac{dN}{dy} dy / \int_0^{y_{beam}} \frac{dN}{dy} dy. \quad (2)$$

The absolute rapidity loss measured by BRAHMS experiment is $\delta y = 2 \pm 0.4$, as it is shown in the right panel in Fig. 5, which is slightly larger than at SPS. But since the over all beam energy is larger at RHIC than at SPS, the absolute energy loss increase appreciately from SPS to RHIC, which results in a significantly increased amount of energy for particle creation at RHIC energies.

We have found that the average energy loss of the colliding nuclei in the most 5% central Au+Au collisions at $\sqrt{s_{NN}} = 200 \text{ GeV}$ is about $73 \pm 6 \text{ GeV}$, which means $\sim 73\%$ of the beam energy is used for particle production.

3.2 Nuclear modification factor

The nuclear modification factor, which is defined as a ratio of the particles yield produced in A+B collision to the particle yield produced in elementary N+N collisions, scaled with the the number of binary collisions N_{coll}^{AB} , is used to study the medium effects. The comparison with p+p results is based in the assumption that the production of moderately high transverse momentum particles scales with the number of binary collisions in the initial stages.

$$R_{AB} = \frac{1}{N_{coll}^{AB}} \frac{N_{AB}(p_T, \eta)}{N_{pp}(p_T, \eta)}. \quad (3)$$

Both d+Au and Au+Au spectra are compared to normalized p+p spectra at the same spectrometer settings in this overview. For comparison to the results obtained for the central Au+Au collisions at $\sqrt{s_{NN}} = 200 \text{ GeV}$, we have investigated the d+Au reaction at the same energy at $\eta = 0$. In Fig. 6, we present the corresponding R_{dAu} distribution in minimum bias collisions, analyzed in the same way as the Au+Au collisions. It is obvious that R_{dAu} shows no suppression of the high p_T component, but an enhancement instead at mid-rapidity, which is similar to the one observed at lower energies [12]. Apparently, the final state jet-quenching plays a more important role in the central Au+Au collisions than that in d+Au collisions, while the initial state multiple scattering effect is more dominant in the d+Au system.

Fig. 7 shows a clear variation of the R_{dAu} as a function of pseudo-rapidity. At mid-rapidity, $R_{dAu} > 1$ evidencing a Cronin enhancement as compared to the binary scaling limit when $p_T > 2.0 \text{ GeV}/c$. This enhancement is attributed to multiple scattering of partons during the collisions resulting in an accumulation of the yield of the final state partons in the p_T range $2 - 5 \text{ GeV}/c$, at the expense of yield at lower p_T . At $\eta = 1$ the Cronin peak is not present and at more forward rapidities ($\eta = 3.2$) the data shows a suppression of the hadron yield. A rise with p_T is observed at all rapidities.

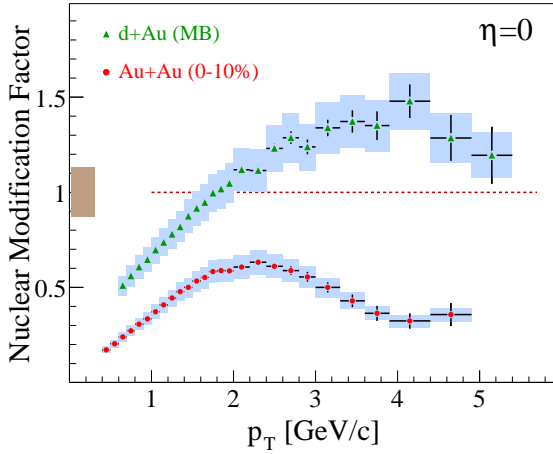


Fig. 6. Nuclear modification factor measured for central (0-10%) Au+Au collisions and minimum bias d+Au collisions at $\sqrt{s_{NN}} = 200 \text{ GeV}$. Error bars represent statistical errors, and the gray band at $p_T = 0$ is the uncertainty caused by the scale of R_{AuAu} .

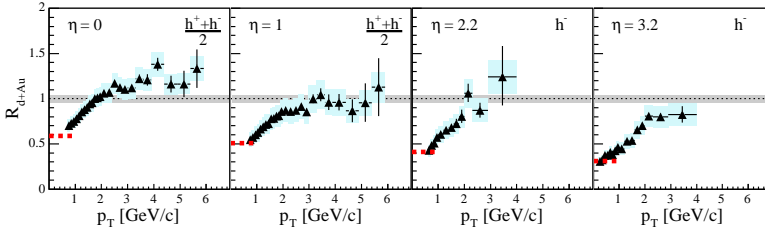


Fig. 7. Nuclear modification factor for charged hadrons at R_{dAu} plots for hadrons pseudo-rapidities at $\eta = 0, 1, 2.2, 3.2$. One standard deviation statistical errors are shown with error bars. Systematic errors are shown with shaded boxes with width set by the bin size. The shaded band around unity indicates the estimated errors on the normalization to $\langle N_{coll} \rangle$. Dashed lines at $p_T < 1 \text{ GeV}/c$ show the normalized charged particle density ratio.

Another variable R_{CP} are constructed as the ratio of R_{AB} in central collisions to that in peripheral collisions, namely

$$R_{CP} = \frac{N_{cen}(p_T, \eta) / N_{coll}^{cen}}{N_{per}(p_T, \eta) / N_{coll}^{per}}. \quad (4)$$

The spectra from the nucleon nucleon collisions are canceled out, which makes it independent on the reference spectra under the assumption that the nuclear

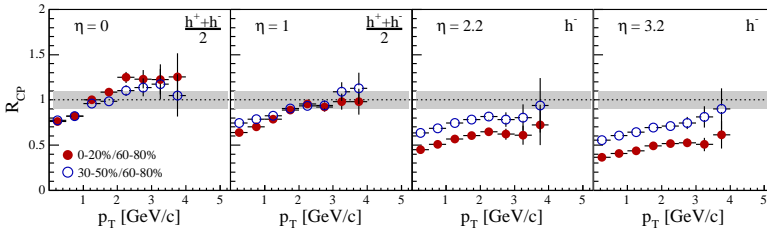


Fig. 8. Central (full points) and semi-central (open points) to peripheral ratios R_{CP} at pseudo-rapidity $\eta = 0, 1.0, 2.2, 3.2$ [13].

modification in peripheral collisions is not significant, so that the deviation from unity of the R_{CP} is dominated by the nuclear effects in the more central collisions.

The four panels of Fig. 8 show the ratio R_{CP} of yields from collisions of a given centrality class (0-20%, 30-50%) to yields from more peripheral collisions (60-80%), scaled by the averaged number of binary collisions in each centrality bin. The centrality selections is based on charged particle multiplicity in the range $-2.2 < \eta < 2.2$ as described in [14]. The averaged numbers of binary collisions used in our analysis are $N_{coll}^{0-20\%} = 13.6 \pm 0.3$, $N_{coll}^{30-50\%} = 7.9 \pm 0.4$ and $N_{coll}^{60-80\%} = 3.3 \pm 0.4$. A substantial change is seen in R_{CP} between $\eta = 0$ and the forward rapidities. At low pseudo-rapidities, the central-to-peripheral ratio is larger than the semi-central-to-peripheral ratio, suggesting the increased role of Cronin multiple scattering effects in the more violent collisions. While at forward pseudo-rapidities, the more central ratio is the more suppressed, indicating a mechanism for suppression which depends on the centrality of the collision.

Fig. 9 shows the energy dependence of the nuclear modification factor for charged hadrons in Au+Au collisions at $\sqrt{s_{NN}} = 200 \text{ GeV}$ at mid-rapidities ($\eta \sim 0, 1$) with different centrality classes, namely 0-10%, 10-20%, 20-40% and 40-60%. We observe that for the most central collisions, R_{AuAu} shows suppressions for both energies, while the the suppression is much stronger for the higher energy and more central collisions. The Cronin enhancement is already seen in the 20-40% semi-central Au+Au collisions at $\sqrt{s_{NN}} = 62.4 \text{ GeV}$, where R_{AuAu} reaches its peak in the p_T range between 2 – 3 GeV/c , suggesting both jet-quenching (dominates at central collisions) and Cronin effect (prevails for more peripheral collisions) are present at this intermediate and high p_T range.

In Fig. 10, we compare the nuclear modification factor for pions and protons at $y \approx 3.2$ measured by BRAHMS with the results from PHENIX experiment at $y = 0$. A very strong suppression is seen for pions at both forward rapidity and mid-rapidity. The similarity between R_{AuAu} at both rapidities for either pions or protons suggests there is no different nuclear modification mechanism between rapidity interval $0 < y < 3.2$.

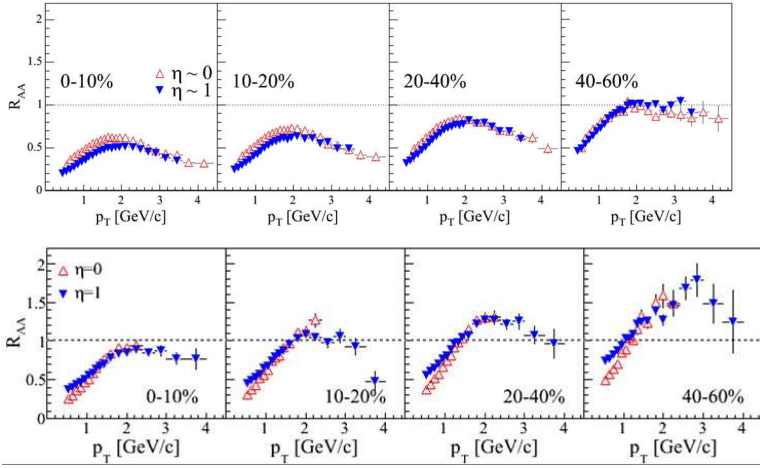


Fig. 9. Comparison of R_{AA} dependence on centrality at different colliding energies: the upper row is for the Au+Au collisions at $\sqrt{s_{NN}} = 200 \text{ GeV}$ and the lower row is for that at 62.4 GeV [15].

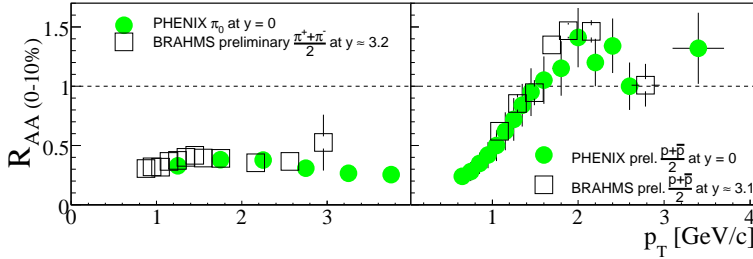


Fig. 10. Comparison if R_{AA} measured for central (0-10%) Au+Au collisions at $\sqrt{s_{NN}} = 200 \text{ GeV}$ at mid-rapidity and $y \approx 3.2$ for pions (left panel) and protons (right panel) [16].

4 Summary and discussions

An overview of the main experimental results obtained by the BRAHMS experiment at Relativistic Heavy Ion Collider (RHIC) for Au+Au collisions at $\sqrt{s_{NN}} = 62.4, 200 \text{ GeV}$ and d+Au collisions at $\sqrt{s_{NN}} = 200 \text{ GeV}$ has been presented.

The m_T spectra and the Gaussian-like rapidity densities of produced pions and kaons in Au+Au central collisions at $\sqrt{s_{NN}} = 200 \text{ GeV}$ are shown, and the rapidity densities are compared with results from models. The analysis of net-proton rapidity density to study the nuclear stopping in the most 5% central Au+Au collisions at

$\sqrt{s_{NN}} = 200 \text{ GeV}$ has demonstrated that about 73% of the participant energy is potentially available for particle production. Landau's full stopping assumption therefore does not hold at RHIC. Bjorken [3] proposed a scenario in which yields of produced particles would be boost-invariant within a region around mid-rapidity. In that approach, reactions are described as highly transparent leading to a vanishing net-baryon density around mid-rapidity and particle production from pair creation from the color field in the central zone. This would result in a flat distribution of particle yields around $y \sim 0$. Collisions at RHIC are neither fully stopped nor fully transparent, although a relatively high degree of transparency is observed [17], corresponding to an average rapidity loss of the colliding hadrons of about $\delta y \approx 2$.

The observed suppression of the charged hadron yield in d+Au collisions as compared to p+p collisions at forward rapidity have been qualitatively predicted by several authors [18, 19, 20] within the framework of gluon saturation that includes the effect of the so called 'quantum evolution' as particles are detected away from mid-rapidity. Other authors [21] have based their predictions of nuclear modification factors on a two component model that includes a parameterization of perturbative QCD and string breaking as a mechanism to account for soft coherent particle production, using the HIJING microscopic event generator [22]. HIJING uses the effect of 'gluon shadowing' as a method of reducing the number of effective gluon-gluon collisions and hence the multiplicity of charged particles at lower p_T , and also includes an explicit cutoff parameter for mini-jet production. The HIJING model has been shown to give a good description of the overall charged particle distribution in d+Au collisions.

We compared the nuclear modification factor for Au+Au at $\sqrt{s_{NN}} = 200 \text{ GeV}$ and $\sqrt{s_{NN}} = 62.4 \text{ GeV}$, the enhancement of R_{AuAu} is stronger at lower energy and in more peripheral collisions, which suggests the final state jet-quenching play main role at higher energy and in more central collisions, while at lower energy and in more peripheral collisions, the initial stage effects are dominated. For Au+Au central collisions at $\sqrt{s_{NN}} = 200 \text{ GeV}$, R_{AuAu} shows very weak dependence on rapidity (in $0 < y < 3.2$ interval), both for pions and protons.

Acknowledgments

This work was supported by the Division of Nuclear Physics of the Office of Science of the U.S. Department of Energy, the Danish Research Council, the Research Council of Norway, the Jagiellonian University Grants, and the Romanian Ministry of Research.

References

- [1] U. Heinz, Nucl. Phys. A **721**, 30 (2003).
- [2] L. D. Landau, Izv. Akad. Nauk, SSSR Ser. Fiz., **17**, 51 (1953).
- [3] J. D. Bjorken, Phys. Rev. D **27**, 140 (1983).
- [4] X.-N. Wang, Phys. Rev. C **58**, 2321 (1998).

- [5] L. McLerran and R. Venugopalan, Phys. Rev. D **49**, 2233 (1994); Phys. Rev. D **59**, 094002 (1999); E. Iancu, A. Leonidov and L. D. McLerran, Nucl. Phys. A **692**, 583 (2001), and references therein.
- [6] M. Adamczyk *et al.*, [BRAHMS Collaboration], Nucl. Inst. Meth. A **499**, 437 (2003).
- [7] I. Arsene *et al.*, [BRAHMS Collaboration], Phys. Rev. Lett. **91** 72305 (2003).
- [8] D. Ouerdane, Ph.D Dissertation, Copenhagen University (DK), August 2003.
- [9] J. L. Klay *et al.* (E895), Phys. Rev. C **68**, 054905 (2003).
- [10] S. V. Afanasiev *et al.* (NA49), Phys. Rev. C **66**, 054902 (2002).
- [11] P. Carruthers and M. Duong-van, Phys. Lett. B, **41**, 597 (1972); Phys. Rev. D **8**, 859 (1973); F. Cooper and E. Schonberg, Phys. Rev. Lett. **30**, 880 (1973).
- [12] H. Appelshauser *et al.*, Phys. Rev. Lett. **82**, 2471 (1999); M. M. Aggarwal *et al.*, Eur. Phys. J. C **18**, 651(2001).
- [13] I. Arsene *et al.*, [BRAHMS Collaboration], Phys. Rev. Lett. **93**, 242303 (2004).
- [14] I. Arsene *et al.*, [BRAHMS Collaboration], Phys. Rev. Lett. **94**, 032301 (2005).
- [15] P. Staszal, for the BRAHMS Collaboration, Proceedings for Quark Matter Conference, Budapest, 2005.
- [16] R. Karabowicz for the BRAHMS Collaboration, Proceedings for Quark Matter Conference, Budapest, 2005.
- [17] I. Arsene *et al.*, [BRAHMS Collaboration], Phys. Rev. Lett. **90**, 102301 (2004).
- [18] D. Kharzeev, Y. V. Kovchegov and K. Tuchin, Phys. Rev. D **68**, 094013 (2003); D. Kharzeev, E. Levin and L. McLerran, Phys. Lett. B **561**, 93 (2003).
- [19] R. Baier, A. Kovner, U. A. Wiedemann, Phys. Rev. D **68**, 054009 (2003); J. L. Albacete, N. Armesto, A. Kovner, C. A. Salgado and U. A. Wiedemann, Phys. Rev. Lett. **92**, 082001 (2004).
- [20] J. Jalilian-Marian, Y. Nara and R. Venugopalan, Phys. Lett. B **577**, 54 (2003); A. Dumitru and J. Jalilian-Marian Phys. Rev. Lett. **89**, 022301 (2002).
- [21] R. Vogt, hep-ph/0405060, Phys. Rev. C in print.
- [22] X.-N. Wang and M. Gyulassy, Phys. Rev. D **44**, 3501 (1991); M. Gyulassy and X.-N. Wang, Comput. Phys. Commun. **83**, 307 (1994).